Acta Physiologiae Plantarum (2018) 40:212
https://doi.org/10.1007/s11738-018-2790-9

ORIGINAL ARTICLE

Root flooding-induced changes in the dynamic dissipation of the photosynthetic energy of common bean plants

Douglas Antônio Posso[1] · Junior Borella[1] · Gabriela Niemeyer Reissig[2] · Marcos Antonio Bacarin[1]

Received: 22 June 2018 / Revised: 5 November 2018 / Accepted: 16 November 2018 / Published online: 21 November 2018

Abstract

In this work, we evaluated changes in the energy dissipation on electron transport chain of photosystems of leaves of four common bean (*Phaseolus vulgaris* L.) genotypes (cultivars and landraces) in response to root system flooding. Common bean plants (BRS Expedito and Iraí—cultivars; TB 02–24 and TB 03–13—landraces) were grown in soil and commercial substrate (1:1). At the early reproductive stages, the root system was subjected to flooding by adding distilled water up to 2 cm above the substrate surface for 4 days. Control plants were kept under normoxia. Chlorophyll *a* fluorescence, gas exchange, photorespiration, antioxidative enzymes and reactive oxygen species (ROS) were measured in leaves on the 4th day of flooding. Flooding of the root system reduced gas exchange in all genotypes with strong effects in CO_2 assimilation. BRS Expedito genotype had a greater energy dissipation through fluorescence and heat over Iraí, TB 02–24 and TB 03–13, with regard of metabolic regulation through photorespiration to alleviate the excess of ATP/NADPH produced by the electron transport chain (ETC). On the other hand, the genotypes Iraí, TB 02–24 and TB 03–13 induced more efficiently the antioxidative enzyme system to cope with the deleterious effects of ROS in comparison to BRS Expedito. Further, the dynamic energy dissipation of the excess absorbed energy by the photosynthetic ETC was differentially dissipated in all four common bean genotypes.

Keywords *Phaseolus vulgaris* L. · Waterlogging · Photosynthesis · Photorespiration · Antioxidative enzyme

Introduction

Common bean (*Phaseolus vulgaris* L.) is one of the most important food legumes that provide as much as 30% of the daily dietary protein in some developing countries for human consumption. However, climate changes are increasing the number of events of soil flooding (Bailey-Serres et al. 2012; Limami et al. 2014), representing a significant threat to food production (USDA 2015). As the oxygen diffusion in water is 10^4 times slower than in air (Armstrong et al. 1994), flooding impairs oxygen supply to the roots, inhibiting root respiration, water uptake, hydraulic conductance, and consequently leads to stomatal closure (Aroca et al. 2012; Limami et al. 2014).

Stomatal closure restricts the diffusion of CO_2 from the air into the carboxylation sites of Rubisco (Aroca et al. 2012; Herrera 2013; Bansal and Srivastava 2015), decreasing the rate of photosynthesis (Mielke and Schaffer 2011), and affecting the flow of energy on electron transport chain (ETC) of photosystems (PS) (Eullaffroy et al. 2009; Santos Junior et al. 2015). However, the ability to maintain the functionality of the ETC machinery under flooding may be different among plant genotypes.

When photosynthesis is suppressed, photorespiration has been reported to contribute to the consumption of excess photon energy and thereby suppress the accumulation of electrons in the photosynthetic electron transport system (Hanawa et al. 2017), which could operate in leaves of common bean to alleviate plants from photoinhibition upon flooding. On the other hand, part of the accumulated electron can flow to oxygen producing reactive oxygen species (ROS) (Foyer et al. 2017). ROS trigger oxidative damage of membrane lipids (causing lipid peroxidation) leading to membrane injuries, protein degradation and enzyme

Communicated by S. Esposito.

✉ Junior Borella
borellaj@gmail.com

[1] Departamento de Botânica, Universidade Federal de Pelotas, C.P. 354, Pelotas, RS 96160-000, Brazil

[2] Departamento de Ciência e Tecnologia Agroindustrial, Universidade Federal de Pelotas, C.P. 354, Pelotas, RS 96160-000, Brazil

inactivation (Gill and Tuteja 2010). To cope with oxidative damage, plants induce an efficient antioxidative defense system (Blokhina and Fagerstedt 2010).

The symptoms of flooding on plants, in general, depend on the soil O_2 partial pressure and besides that, plant species or even genotypes presented a wide variation in their ability to respond the oxygen deprivation through a series of several adaptive mechanisms as a strategy to avoid or postpone the effects caused by hypoxia to ensure their survival (Bailey-Serres et al. 2012; Kreuzwieser and Rennenberg 2014; Borella et al. 2017). However, many of these variations in plant species or genotypes are related to changes in carbon and nitrogen metabolism under hypoxia. (Rocha et al. 2010; António et al. 2016; Borella et al. 2017).

In this sense, plant genotypes may use a different way to dissipate the excess of energy trapped on photosystems to alleviate the effects caused by flooding. The effects of low oxygen availability due to root flooding on the photosynthetic metabolism of common bean plants are scarce, irrespective of how different genotypes respond to it. Therefore, the aim of this study was to investigate how the electron transport chain of photosystems drives the flow of the absorbed energy in leaves of four common bean genotypes (cultivars and landraces) in response to root system flooding.

Materials and methods

Plant material and growth conditions

Common bean plants (*Phaseolus vulgaris* L.) of four genotypes (BRS Expedito and Iraí—cultivars; TB 02–24 and TB 03–13—landraces) were grown in a greenhouse under natural light (± 1.000 µmol photons m^{-2} s^{-1}) and temperature conditions (25 ± 5 °C), previously characterized by our group as having high (BRS Expedito and TB 02–24) and low (Iraí and TB 03–13) photosynthetic efficiency among a genotype screening under normoxic conditions (data not shown). One plant of each common bean genotype was grown in a single plastic pot (1 L) containing soil and commercial substrate (1:1) and supplied with 20 mL of nutrient solution three times per week (Hoagland and Arnon 1938). When plants reached the R1 stage (flowering—early reproductive stage; see Osorno et al. 2014), flooding treatment was carried out by adding distilled water into the plastic pot up to reach 2 cm of water above the substrate surface, to keep the whole root system submersed (control plants were kept under normoxic conditions). During 4 days of flooding (period previously selected due to the sensitivity of common bean plants to flooding—data not shown), physiological parameters were measured daily and at the fourth day leaves were collected for each plant genotype and kept frozen (−80 °C) until analysis (all analyses were performed in the fully expanded first trifoliate leaf).

Chlorophyll index

Chlorophyll index was measured as described by Cassol et al. (2008), with a portable chlorophyll meter (CL-01; Hansatech Instruments, King's Lynn, Norfolk, UK). The measurements were taken from the fully expanded first trifoliate leaf.

Measurements of chlorophyll *a* fluorescence transients

Chlorophyll *a* fluorescence transients were measured in dark-adapted leaf of plants with a Handy-PEA fluorimeter (Plant Efficiency Analyser, Hansatech Instruments Ltd, UK). The measurements were done in intact young leaves (fully expanded first trifoliate leaf) still attached to the plant and kept in the dark for at least 30 min in specially provided clips. The polyphasic fluorescence rise, OJIP, was induced by one saturating red-light flash (peak at 650 nm) with 3.000 µmol photons m^{-2} s^{-1} and measured during the first second of illumination (10 µs to 1 s). The OJIP fluorescence transients are based on the polyphasic fast fluorescence rise from the lowest intensity F_O (minimum fluorescence) to the highest intensity F_M (maximum fluorescence) (Strasser and Tsimilli-Michael 2004). The O-step is the initial fluorescence level (50 µs), J (2 ms) and I (30 ms) are intermediate levels, and P (500 ms–1 s) is the peak level, analysed using the JIP test parameters (For analysis of Chl fluorescence data see Strasser et al. (2004) and Tsimilli-Michael and Strasser (2008). The intensity measured at 50 µs was considered as the initial fluorescence (F_0). The plotted fluorescence values were the average of ten measurements of each treatment.

The JIP test was also applied for the analysis and comparison of the OJIP transients using normalizations and subtractions to compare the samples for the events reflected in the OJ, OI, and IP phases. The transients were normalized as relative variable fluorescence: $W_{OJ} = (F_t - F_0)/(F_J - F_0)$, $W_{OI} = (F_t - F_0)/(F_I - F_0)$ and $W_{IP} = (F_t - F_I)/(F_P - F_I)$. In addition, difference kinetics from relative variable fluorescence data were also calculated ($\Delta W = W_{flooded} - W_{control}$), which reveals hidden bands between the steps W_{OJ} (K-band; 300 µs) and W_{OK} (L-band; 150 µs) according to Yusuf et al. (2010).

Gas exchange measurements

Gas exchange was measured in intact young leaves (fully expanded first trifoliate leaf) still attached to the plant with a portable infra-red CO_2 analyser (model LI-6400XT LI-COR, Inc., Lincoln, NE, USA). The measurements were taken

between 10:00 and 11:00 AM, with an in-chamber CO_2 concentration of 380 µmol mol^{-1} and a photon flow density of 1.250 µmol photons m^{-2} s^{-1}, using the light source LI-COR 6400-02B attached to the measuring chamber (2 × 3 cm) with a block temperature control set up at 25 °C.

Glycolate oxidase activity

Glycolate oxidase (GO—EC 1.1.3.1) activity was assayed as described by Bai et al. (2014). Fresh leaf tissue (± 0.2 g) was ground to a powder using a mortar and pestle with liquid nitrogen and homogenized with 5% polyvinylpolypyrrolidone (PVPP) and 50 mM Tris–HCl buffer (pH 7.8) containing 0.01% Triton X-100 and 5 mM dithiothreitol (DTT). The homogenate was centrifuged at 12 000 *g* for 20 min at 4 °C and the supernatant used to measure GO activity which was assayed by following the formation of glyoxylate phenylhydrazone at 324 nm recorded at 10 s intervals in a medium reaction containing 50 mM Tris–HCl (pH 7.8), 0.009% Triton X-100 (v/v), 3.3 mM phenylhydrazone HCl (pH 6.8) and 5 mM glycolate (pH 7.0).

Hydrogen peroxide content and lipid peroxidation measurements

Leaves (± 0.2 g) were ground to a powder using a mortar and pestle with liquid nitrogen and homogenized with 0.1% (*w:v*) trichloroacetic acid (TCA). The homogenate was centrifuged (12 000 *g*, 4 °C, 20 min) and the supernatant was used for the analyses as described by Velikova et al. (2000). Lipid peroxidation was determined according to Cakmak and Horst (1991), using thiobarbituric acid (TBA), which determines malondialdehyde (MDA) as an end product of lipid peroxidation. The amount of MDA–TBA complex (red pigment) was calculated from the extinction coefficient ($\varepsilon = 155 \times 10^3$ M^{-1} cm^{-1}).

Antioxidative enzyme activity

For the measurement of enzyme activities, leaves (± 0.2 g) were ground to a powder using a mortar and pestle with liquid nitrogen and homogenized with 5% (*w:v*) polyvinylpolypyrrolidone (PVPP) and 100 mM potassium phosphate buffer, pH 7.8, containing 0.1 mM ethylenediaminetetraacetic acid (EDTA) and 20 mM sodium ascorbate. The homogenate was centrifuged at 12 000 *g* (20 min at 4 °C), and the supernatant obtained was used as a crude enzyme extract (Azevedo Neto et al. 2006). Superoxide dismutase (SOD—EC 1.15.1.1) activity was assayed by monitoring the inhibition of the nitro blue tetrazolium (NBT) coloration at 560 nm. Catalase (CAT—EC 1.11.1.6) activity was assayed by monitoring the decline in the absorbance at 240 nm. Ascorbate peroxidase (APX—EC 1.11.1.11) activity was assayed through ascorbate oxidation at 290 nm. Guaiacol peroxidase (GPOD 1.11.1.7) activity was assayed by monitoring the tetraguaiacol production at 470 nm.

Statistical analysis

Each treatment consisted of a minimum of four biological replicates for each common bean genotype (cultivar or landrace; the number of biological replicates is indicated in the figure subtitle), in a fully randomized design. Chlorophyll *a* fluorescence was analysed as described above and all other data were analysed by one-way analysis of variance (ANOVA). When *F* was significant, the treatment means for each genotype (control and flooded) and the genotypes in each group (cultivars—BRS Expedito and Iraí; landraces—TB 02–24 and TB 03–13) were compared by *t* test ($p \leq 0.05$). Statistical analyses were performed using the SAS 9.0 statistical software program (SAS Institute Inc. Cary, NC, USA).

Results

Chlorophyll index

4 days of flooding induced a reduction in Chl index in all four common bean genotypes (BRS Expedito and Iraí—cultivars, Fig. 1a; TB 02–24 and TB 03–13—landraces, Fig. 1b). The reduction in Chl index was higher in BRS Expedito (75%) in relation to control, compared to other common bean genotypes which the reduction ranged about 60% in relation to its respective control (Fig. 1).

Chlorophyll *a* fluorescence transients analysis

Chl *a* fluorescence transients measured from the dark-adapted leaves of common bean plants are shown from 50 µs up to 1 s (on logarithmic time scale), in Fig. 2a, b. All common bean genotypes exhibited a typical polyphasic Chl *a* fluorescence OJIP (W_t) transients (the $O_{50\mu s}$, J_{2ms}, I_{30ms} and P_{1s} steps are marked in the plot) under normoxic conditions (control), rising from initial fluorescence (F_O) to maximum fluorescence (F_M). However, plants under flooding conditions showed a marked increase in the curves of relative variable fluorescence at the J and I-steps (2 and 30 ms, respectively), with the most induction of fluorescence at J-step and the loss of shape curve in BRS Expedito (Fig. 2a) in comparison to all others common bean genotypes.

The biophysical fluorescence transients depicted in Fig. 2c and d, were analysed by the JIP test to deduce functional and structural parameters of the photosynthetic behaviour of the plants subjected to hypoxia (energy distribution in the photosynthetic apparatus) (Strasser and Strasser 1995; Strasser et al. 2004). All parameters were normalized to their

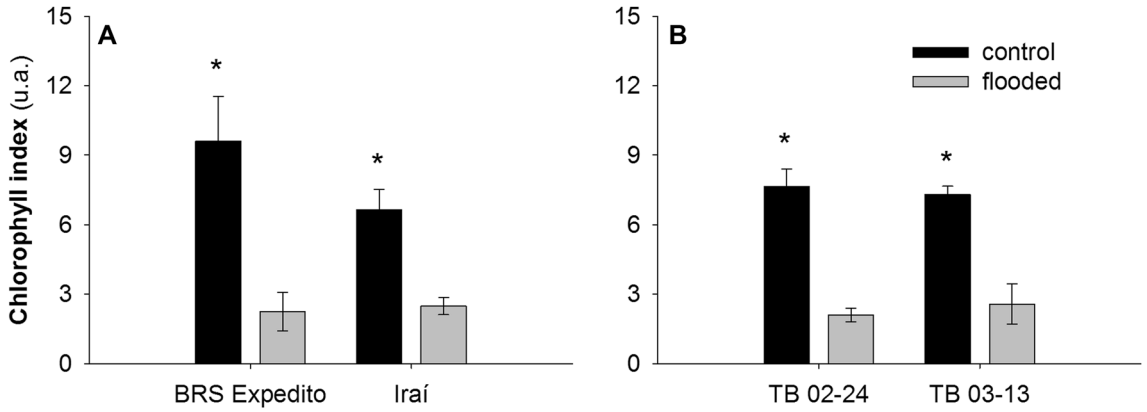

Fig. 1 Chlorophyll index of leaves of four common bean genotypes (**a** BRS Expedito and Iraí cultivars; **b** TB 02–24 and TB 03–13 landraces) subjected to flooding of the root system. *Significant differences by *t* test ($p \leq 0.05$) between control and flooded for each common bean genotype. #Significant differences by *t* test ($p \leq 0.05$) between the genotypes. Values represent the mean ± SD ($n = 4$)

respective control. The sequence of parameters, referring to the sequential energy transduction indicated per RC (Reaction Centre), the energy fluxes for (light) absorption (ABS/RC), trapping (TP_0/RC), heat (DI_0/RC), electron transport (ET_0/RC) and reduction of the end electron acceptors at the PSI acceptor side (RE_0/RC). A similar increase in ABS/RC which measures the apparent antenna size (total absorption or total Chl per active RC), TP_0/RC which measures the energy trapping flux per active RC, able to lead a Q_A reduction (Fig. 2c, d), and DI_0/RC that measures the heat dissipated per RC (data not shown). However, the highest increase in both ABS/RC (about twofold higher) and DI_0/RC (about threefold higher) was in BRS Expedito upon flooding, in comparison to control. Regarding the electron transport flux (further than Q_A^-) per RC (EC_0/RC) and electron flux reducing end electron acceptors at the PSI acceptor side per RC (ET_0/RC) of all plants under flooding were close to the control, except for EC_0/RC that decreased in BRS Expedito compared to the control (Fig. 1c, d).

Decrease in quantum yields and efficiencies of all common bean plants were also observed under flooding in comparison to control (Fig. 2c, d) for maximum quantum yield for primary photochemistry (φ_{Po}), efficiency/probability for electron transport (ET), i.e., efficiency/probability that an electron moves further than Q_A^- (ψ_{Eo}), quantum yield for electron transport (φ_{Eo}) and quantum yield for reduction of end electron acceptors at the PSI acceptor side (RE) (φ_{Ro}). On the other hand, the efficiency/probability with which an electron from the intersystem electron carriers moves to reduce end electron acceptors at the PSI acceptor side (RE) (δ_{Ro}) increased in BRS Expedito, while it was similar in all others common bean plants compared to the control. Regarding the performance indexes, the performance index (potential) for energy conservation from exciton to the reduction of intersystem electron acceptors (PI_{ABS}) and performance index (potential) for energy conservation from exciton to the reduction of PSI end acceptors (PI_{total}) were lower in relation to the control of all common bean plants under flooding (Fig. 2c, d), indicating a reduction in the functionality of the electron transport chain.

When Chl *a* fluorescence data were normalized between the steps O (50 µs) and I (30 ms) and presented as relative variable fluorescence (W_{OI}), we observed an increase in the curves that serves to distinguish the sequence of events from exciton trapping by PSII up to plastoquinone (PQ) reduction (Fig. 3a, b), with the most increase in plants from BRS Expedito under flooding, compared to the control. Figure 3c, d shows the sequence of events from the PSI-driven electron transfer to the end electron acceptors on the PSI acceptor side, starting at PQH_2 (plastoquinol) (W_{IP}), which has decreased in BRS Expedito while remained similar to the control in Iraí and TB 03–13.

To evaluate the kinetics differences between the treatments, we employed additional normalizations and corresponding subtractions between the steps O (50 µs) and K (300 µs) (ΔW_{OK}), to reveal the presence of L-band and between the steps O (50 µs) and J (2 ms) (ΔW_{OJ}), to reveal the presence of K-band. The presence of positive L-band in all common bean plants with the strongest effect of flooding in BRS Expedito (Fig. 3e, f), indicates a low energetic connectivity and an inefficient consumption of the excitation energy and low stability of the system as much as positive L-band is higher (Yusuf et al. 2010). The presence of positive K-band in plants subjected to flooding (Fig. 3g, h), could mean that the oxygen-evolving complex (OEC) becomes leaky and offers access to non-water electron donors evidenced by a decreased reduction rate of quinone (Q_A), the primary electron acceptor of PSII, from Q_A to Q_A^-.

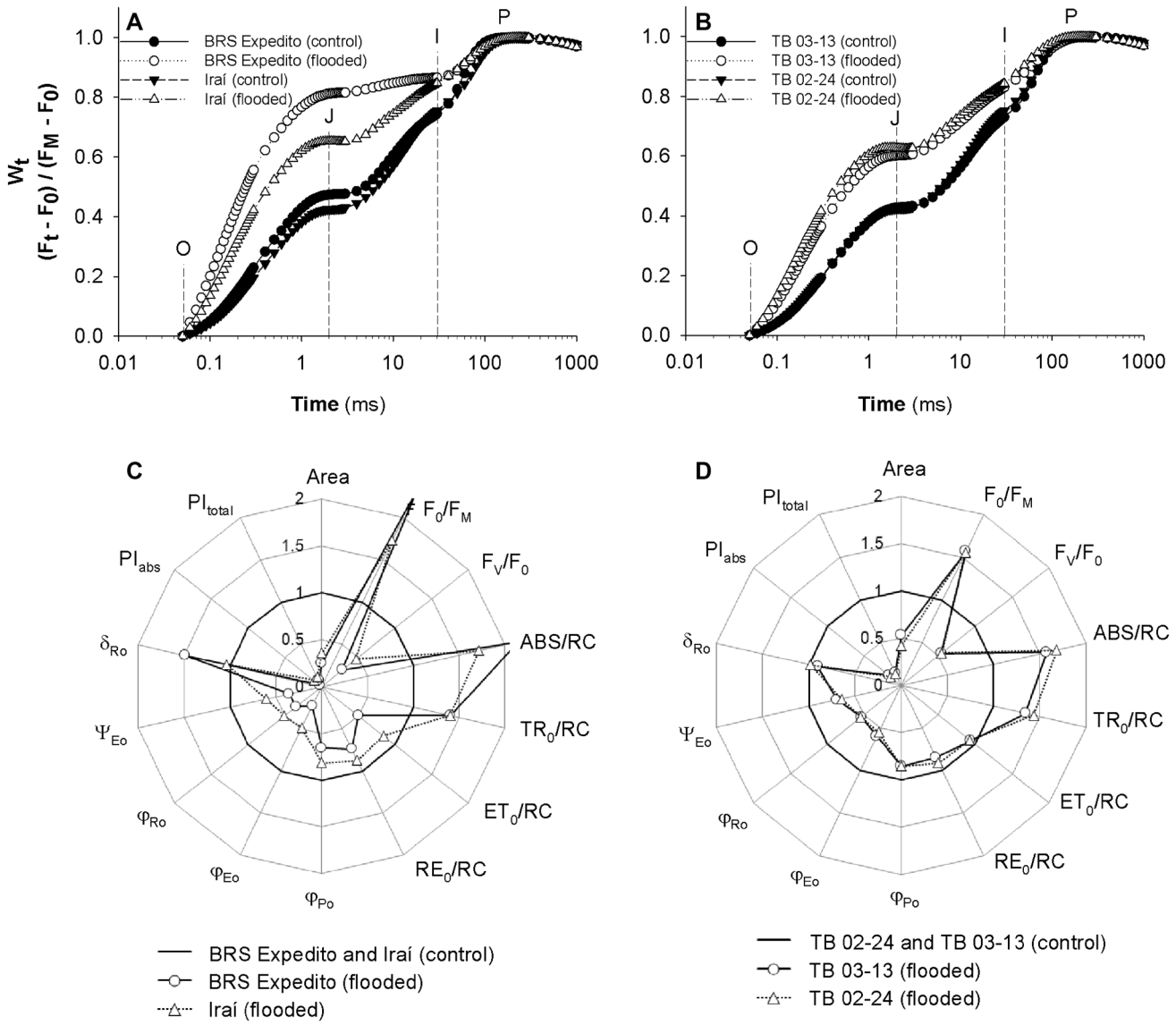

Fig. 2 Chl *a* fluorescence transients (OJIP) of dark-adapted leaves of four common bean genotypes (**a, c** BRS Expedito and Iraí cultivars; **b, d** TB 02–24 and TB 03–13 landraces) subjected to flooding of the root system. **a, b** Relative variable fluorescence between the steps O and P (W_t) on logarithmic time scale; **c, d** Photosynthetic parameters deduced by the JIP test analysis of fluorescence transients normalized using as reference the control ($n = 15$)

Gas exchange under flooding conditions

Net assimilation rate (*A*—Fig. 4a, b) upon 4 days of flooding decreased substantially in all common bean plants (cultivars and landraces), reaching negative values. The reduction in CO_2 assimilation was the result of an expressive reduction in stomatal conductance (g_s—Fig. 4c, d), and transpiration rate (*E*—Fig. 4g, h), the reduction in the genotype BRS Expedito being more expressive when compared to its respective control. On the other hand, intercellular CO_2 concentration (C_i—Fig. 4e, f) increased about twofold higher in all common bean genotypes under flooding conditions.

Effect of flooding on glycolate oxidase enzyme activity

The activity of glycolate oxidase (GO) was interestingly different in all common bean plants (genotypes and landraces). An expressive reduction (threefold) of GO activity was showed by the genotype Iraí, while in BRS Expedito the activity of GO remained close to the activity of the control (Fig. 5a). GO activity decreased also in both common bean landraces (TB 02–24 and TB 03–13; Fig. 5b), however, the reduction was less expressive than in Iraí.

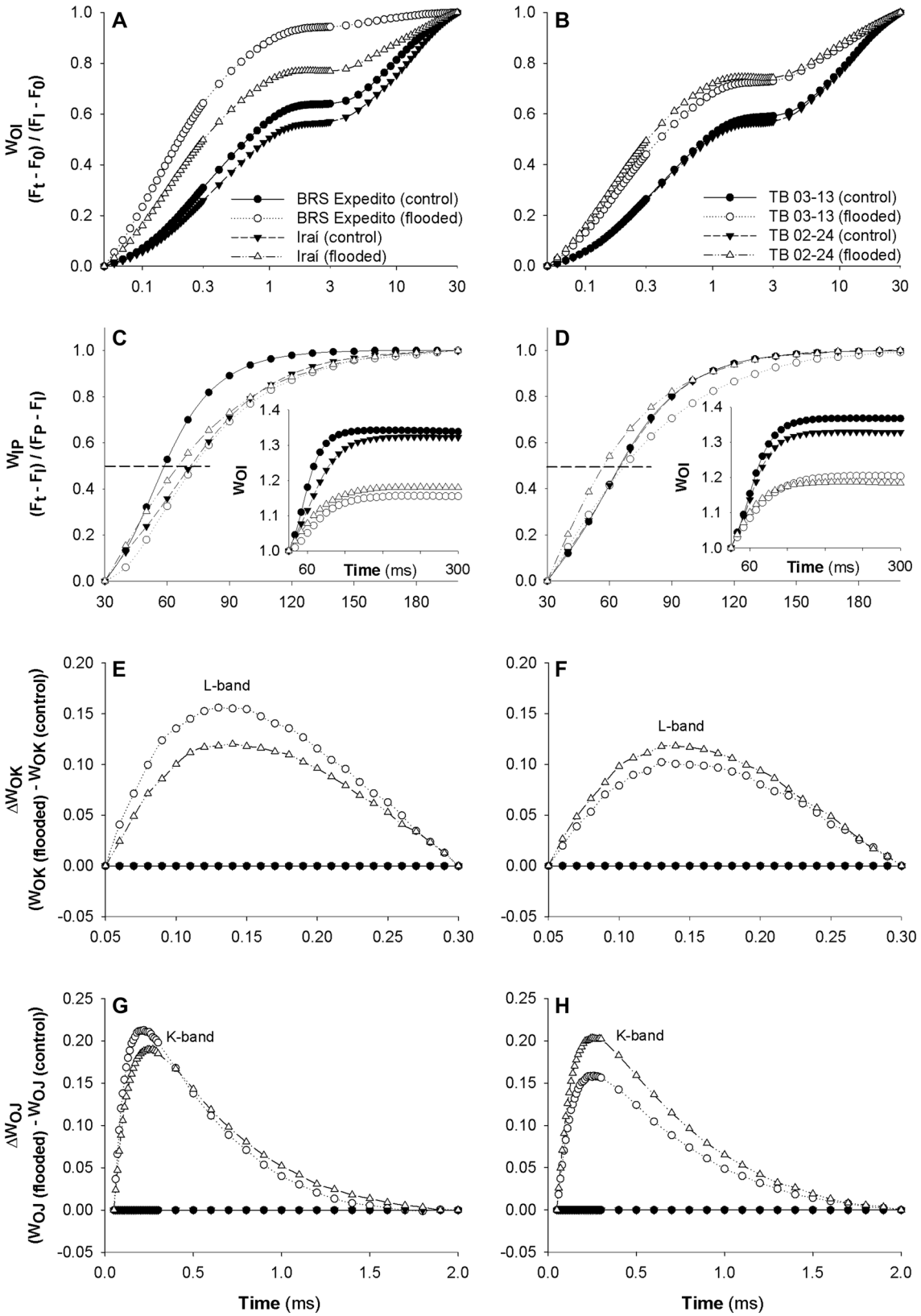
A
B
C
D
E
F
G
H
BRS Expedito (control)
BRS Expedito (flooded)
Irai (control)
Irai (flooded)
TB 03-13 (control)
TB 03-13 (flooded)
TB 02-24 (control)
TB 02-24 (flooded)
L-band
K-band
Time (ms)
Time (ms)

◂**Fig. 3** Chl *a* fluorescence transients (OJIP) of dark-adapted leaves of four common bean genotypes (**a, c, e**, and **g** BRS Expedito and Iraí cultivars; **b, d, f**, and **h** TB 02–24 and TB 03–13 landraces) subjected to flooding of the root system. **a, b** Relative variable fluorescence between the steps O and I (W_{OI}); **c, d** relative variable fluorescence between the steps I and P (W_{IP}) and W_{OI} in the inset; **a, b** on logarithmic time scale; **e, f** average kinetics between the steps O and K (ΔW_{OK}); **g, h** average kinetics between the steps O and J (ΔW_{OJ}); ($n = 15$)

Oxidative stress under flooding

The content of hydrogen peroxide was about twofold higher in leaves of all common bean plants under flooding in comparison to their respective control (Fig. 6a, b). Similarly, there was a significant increase in lipid peroxidation (about twofold higher) in leaves of plants subjected to flooding of the root system, in all common bean plants (Fig. 6c, d).

Effect of flooding on the activity of antioxidative enzymes

Different response to the induction of antioxidative enzyme in leaves of common bean upon flooding is presented in Fig. 7. SOD activity increased significantly in all common bean plants (twofold) in comparison to control, except in BRS Expedito (Fig. 7a, b). On the other hand, CAT activity showed a slight increase only in Iraí, while it decreased in BRS Expedito and TB 02–24 (Fig. 7c, d). In a similar way of SOD, the enzymes APX (Fig. 7e, f) and GPOD (Fig. 7g, h) increased significantly in all common bean plants, with the strongest induction in the genotype Iraí compared to plants under normoxic conditions. Intriguingly, the enzyme CAT showed to be not so responsive to flooding in comparison with other enzymes.

Discussion

Low oxygen availability due to soil flooding inhibits root respiration and leads to a change in carbon and nitrogen metabolism with a considerable decrease in ATP production (Rocha et al. 2010; Kreuzwieser and Rennenberg 2014; van Dongen and Licausi 2015; António et al. 2016). Consequently, water uptake and hydraulic conductance from root to shoot are impaired, affecting photosynthetic metabolism (Aroca et al. 2012; Herrera 2013; Bansal and Srivastava 2015). Under these conditions, changes in the dynamic dissipation of the photosynthetic energy are initiated by plants/genotypes as a mechanism to alleviate the consequences of low oxygen concentrations imposed by flooding to the root system (Herrera 2013; Santos Junior et al. 2015). Consequently, the impairment in the ETC leads to ROS production and the activation of the enzymatic and non-enzymatic system to counteract the effects caused by ROS (Blokhina and Fagerstedt 2010; Aydogan et al. 2015). However, the specific changes in electron transport chain (ETC) and the extent to which they occur may differ among the genotypes subjected to flooding as observed in both group of plants (BRS Expedito and Iraí—cultivars; TB 02–24 and TB03-13—landraces) here studied (Figs. 1, 2, 3, 4, 5, 6, 7).

Different responses were evidenced initially with chlorophyll content (Fig. 1) and chlorophyll *a* fluorescence analysis (Figs. 2, 3). The reduction in chlorophyll content in all genotypes may be related to a decline in mineral nutrient absorption and transport through xylem sap to the shoot, especially nitrogen compounds (Lanza et a. 2014), for chlorophyll biosynthesis. Consequently, the decline in Chl content leads to an impairment in photosynthetic ETC, increasing fluorescence and heat in the genotypes (Fig. 2) and affecting photosynthetic metabolism (Fig. 4) in plants under flooding of the root system.

Chlorophyll *a* fluorescence analysis, normalized as the relative variable fluorescence curve and the calculation of the parameters of the JIP test (Strasser and Strasser 1995; Strasser et al. 2004), demonstrated in BRS Expedito a higher accumulation of Q_A^- (OJ-phase; Fig. 2a) and thermal dissipation of latent heat (JI-phase; Fig. 2a), which are associated with the blockage of ETC further than Q_A^- (Strasser et al. 2004; Yusuf et al. 2010), and resulting in an increase in fluorescence emission (W_t) in comparison to that observed in the three others common bean genotypes (Iraí, TB 02–24 and TB 03–13) under flooding conditions (Fig. 2a, b).

Plants of BRS Expedito also presented a higher quantum yield dissipation (F_0/F_M) among the studied common bean genotypes, which can be a result of the ETC blockage and high specific absorption flow (functional size of the antenna system) per active reaction centre (ABS/RC), leading to an increase in the specific energy dissipation flux per active reaction centre (DI_0/RC) not used in the photochemical reactions and dissipated as heat and/or fluorescence. This differential response between BRS Expedito and the other genotypes was a mechanism to dissipate the excess of energy once there was a similar maximum electron trapping rate per reaction centre (TR_0/RC). In addition, the blockage in the ETC causes a reduction in the transport of electrons further than Q_A^- (electron transport flux—ET_0/RC) to reduce end electron acceptors at the PSI acceptor side per RC (RE_0/RC) due to an impairment caused by the root flooding (Fig. 2c, d). Santos Junior et al. (2015) described that the increase of the antenna system size (ABS/RC) in species under flooding results in decrease in ET_0/RC, as observed in all genotypes here studied with regard to strong effects in BRS Expedito.

An increase of ABS/RC (Fig. 2c, d), which is a measure of the apparent antenna size (which represents the total absorption or total Chl per active RC), may either suggest that a fraction of RCs in the genotypes are inactivated by

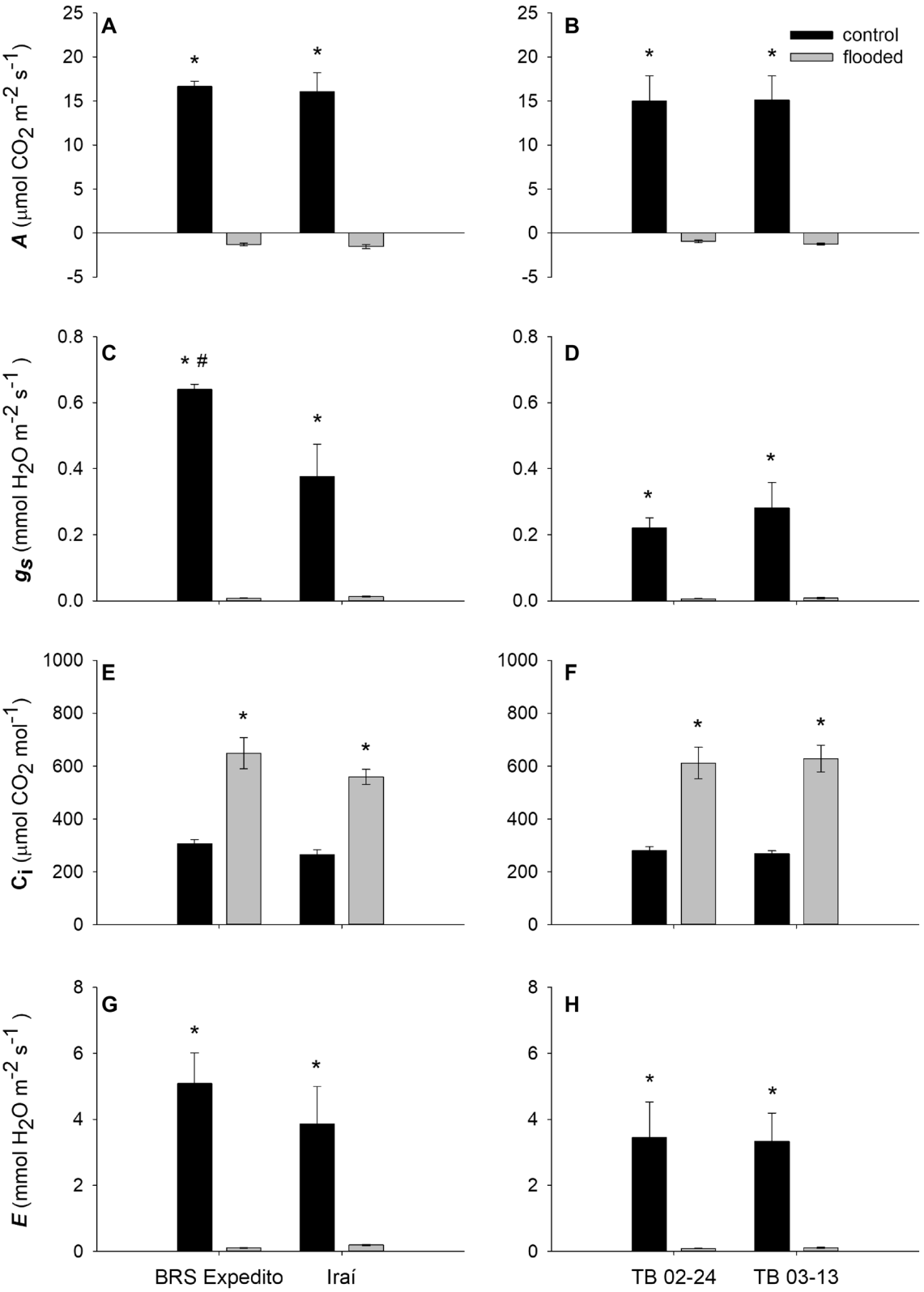

Fig. 4 Gas exchange in leaves of four common bean genotypes (**a, c, e**, and **g**—BRS Expedito and Iraí cultivars; **b, d, f**, and **h**—TB 02–24 and TB 03–13 landraces) subjected to flooding of the root system. *A*—net assimilation rate (**a, b**); g_s—stomatal conductance (**c, d**); C_i—intercellular CO_2 concentration (**e, f**); *E*—transpiration rate (**g, h**). *Significant differences by *t* test ($p \leq 0.05$) between control and flooded for each common bean genotype. #Significant differences by *t* test ($p \leq 0.05$) between the genotypes. Values represent the mean ± SD ($n = 4$)

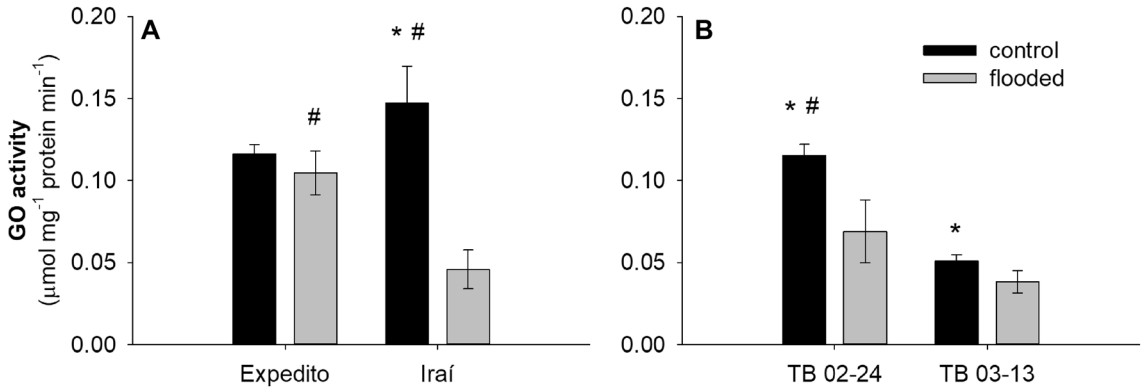

Fig. 5 Glycolate oxidase (GO) activity in leaves of four common bean genotype (**a** BRS Expedito and Iraí cultivars; **b** TB 02–24 and TB 03–13 landraces) subjected to flooding of the root system. *Significant differences by *t* test ($p \leq 0.05$) between control and flooded for each common bean genotype. #Significant differences by *t* test ($p \leq 0.05$) between the genotypes. Values represent the mean ± SD ($n = 4$)

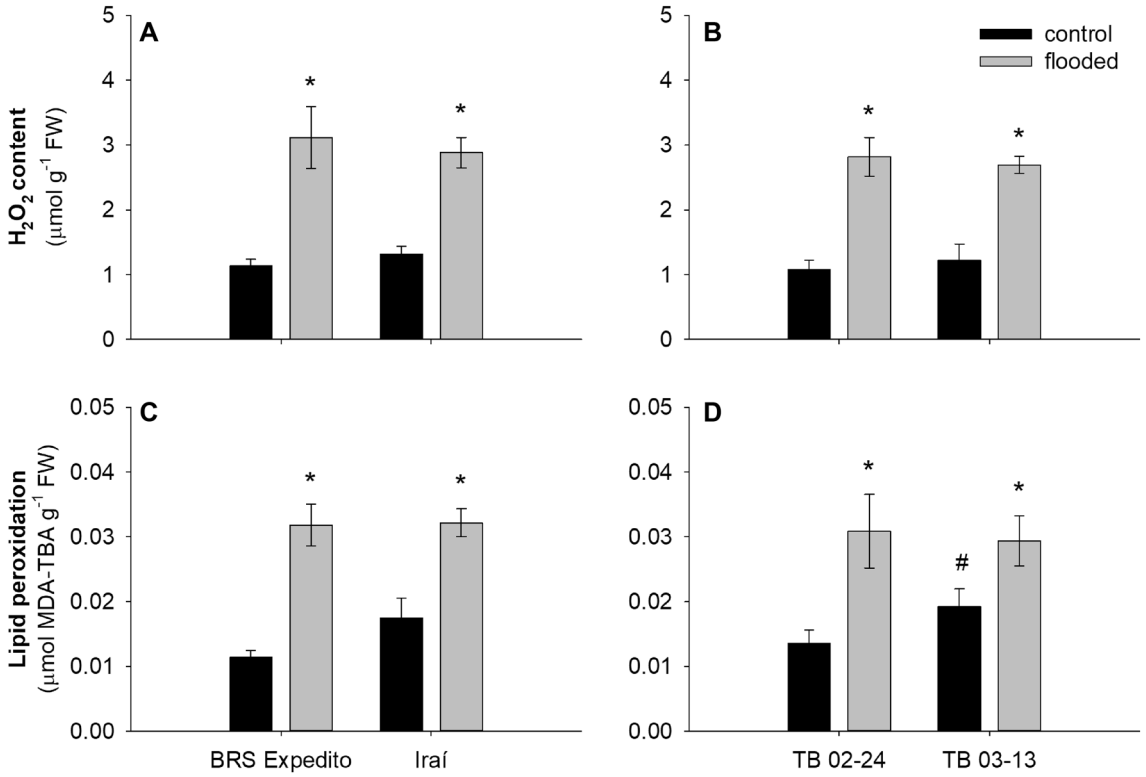

Fig. 6 Hydrogen peroxide content (H_2O_2—**a, b**) and lipid peroxidation (**c, d**) in leaves of four common bean genotypes (**a** and **c** BRS Expedito and Iraí cultivars; **b** and **d** TB 02–24 and TB 03–13 landraces) subjected to flooding of the root system. *Significant differences by *t* test ($p \leq 0.05$) between control and flooded for each common bean genotype. #Significant differences by *t* test ($p \leq 0.05$) between the genotypes. Values represent the mean ± SD ($n = 4$)

being transformed to non-Q_A^- reducing centres or the functional antenna that supplies excitation energy to active RCs has increased in size as reported by Yusuf et al. (2010). On the other hand, an increase in ABS/RC does not lead to an increase in ET_0 and RE_0/RC (Fig. 2c, d) to produce reducing power due to the impairment in CO_2 assimilation caused by a reduction in leaf gas exchange (Fig. 4) as evidenced in all four common bean genotypes under root flooding conditions.

Besides the specific energy fluxes per RC, a similar effect in the genotypes were found for quantum yields and efficiencies in plants subjected to flooding with higher negative effects in BRS Expedito, where, there were a reduction in

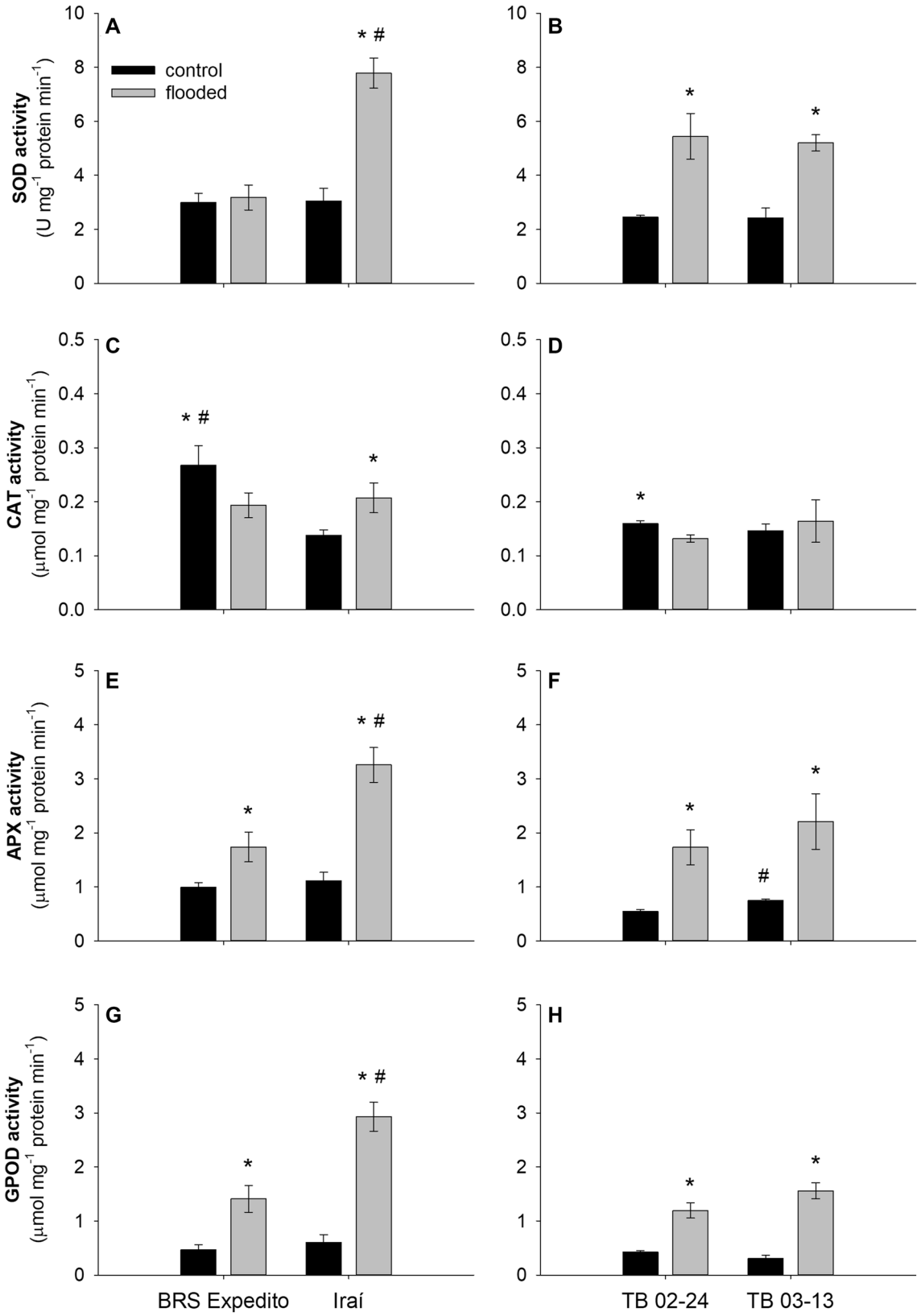
A
B
C
D
E
F
G
H
control
flooded
SOD activity
(U mg-1 protein min-1)
CAT activity
(µmol mg-1 protein min-1)
APX activity
(µmol mg-1 protein min-1)
GPOD activity
(µmol mg-1 protein min-1)
BRS Expedito
Iraí
TB 02-24
TB 03-13

◂**Fig. 7** Antioxidative enzyme activity in leaves of four common bean genotype (**a, c, e**, and **g** BRS Expedito and Iraí cultivars; **b, d, f**, and **h** TB 02–24 and TB 03–13 landraces) subjected to flooding of the root system. *SOD* superoxide dismutase (**a, b**), *CAT* catalase (**c, d**), *APX* ascorbate peroxidase (**e, f**), *GPOD* guaiacol peroxidase (**g, h**). *Significant differences by *t* test ($p \leq 0.05$) between control and flooded for each common bean genotype. #Significant differences by *t* test ($p \leq 0.05$) between the genotypes. Values represent the mean ± SD ($n = 4$)

maximum quantum yield for primary photochemistry (ϕ_{Po}), quantum yield for electron transport (ϕ_{Eo}), quantum yield for reduction of end electron acceptors at the PSI acceptor side (ϕ_{Ro}), efficiency/probability for electron transport, i.e., efficiency/probability that an electron moves further than Q_A^- (Ψ_{Eo}) (Fig. 2c, d) as a result of the blockage in electron transport (ET) in the ETC. On the other hand, a decrease in ET leads to an increase in the efficiency/probability with which an electron from the intersystem electron carriers moves to reduce end electron acceptors at the PSI acceptor side though it did not result in increase in ϕ_{Ro} and RE_0/RC, which probably influenced in lower NADPH and ATP production (Strasser and Strasser 1995; Strasser et al. 2004; Yusuf et al. 2010). Decrease in NADPH and ATP production is associated with decrease in CO_2 assimilation (Fig. 4) by Rubisco and the excess of the reducing power and adenylate energy charge is dissipated through photorespiration as evidenced in the BRS Expedito genotype (Fig. 5).

The performance indexes (PI_{ABS} and PI_{total}), that describe the operation of the electron transport chain from the absorption of the photon to the reduction of the PSI final acceptors (Tsmilli-Michael and Strasser 2008) were highly reduced in all common bean genotypes (Fig. 2c, d) under flooding. Reductions in performance indexes are correlated to a decrease in density of the reaction centre, capture efficiency, and electron transport efficiency under root flooding evidencing a lower functionality of the electron transport chain compared to plants under normoxia (Fig. 2c, d).

To support the effects of the root flooding on photosynthetic ETC, fluorescence data were normalized between the steps O (50 µs) and I (30 ms) and presented as relative variable fluorescence (W_{OI}), where an increase was evidenced in the sequence of events from exciton trapping by PSII up to plastoquinone (PQ) reduction (O–I phase; W_{OI} from 0 to 1; Fig. 3a, b), as showed by an increase in TR_0/RC (Fig. 2). On the other hand, reduction in ET_0/RC caused reduction in the PSI-driven electron transfer to the end electron acceptors on the PSI acceptor side, starting at PQH_2 (plastoquinol) (I–P phases; $W_{OI} \geq 1$, insert graph in the Fig. 3c, d), in all four common bean genotypes subjected to flooding in comparison to plants under normóxia conditions. In the main plot (Fig. 3c, d), fluorescence normalized as I–P phase, the reduction of the end electron acceptor was lower in BRS Expedito in comparison to its respective control and in relation to the results showed by the other genotypes, as demonstrated by RE_0/RC (Fig. 2c, d), which may lead to a decline in NADPH and ATP production.

Reduction of the energy connectivity of PSII [indicated by the presence of the positive L-band; normalized between the steps O (50 µs) and K (300 µs), as W_{OK}], was more accentuated in the genotype BRS Expedito which implies in lower system stability and lower energy utilization (Fig. 3e, f), reducing the efficiency with which absorbed energy is transmitted between PSII units (Tsimilli-Michael and Strasser 2008), increasing the dissipation of the energy absorbed via heat (data not shown) and fluorescence (Fig. 2) as reported by Stirbet and Govindjee (2011) and Santos Junior et al. (2015). The presence of positive K-band [normalized between the steps O and J (2 ms), as W_{OJ}] in flooded plants (Fig. 3g, h), reflects either an increase of the functional PSII antenna size, and/or an inactivation of the oxygen-evolving complex (Yan et al. 2013), as evidenced by an increase in ABS/RC (Fig. 2c, d) in all genotypes.

Damage to the oxygen-evolving complex leads to an imbalance in the energy flux in PSII, increasing the time of excited states of chlorophyll molecules from the reaction centre of the photosystem, which increases the probability of singlet oxygen ($^1O_2$) formation and, consequently photooxidative damage (Foyer et al. 2017). In addition, reduction in the functionality of the ETC caused by flooding limits the production of NADPH and a reduction in the net assimilation rate of CO_2 (A; Fig. 4a, b). This fact is associated with reduction in gas exchange caused by stomatal closure and reduction in transpiration rate (E; Fig. 4g, h) also reported by Bansal and Srivastava (2015), due to reduction on water absorption by roots and transport of water through xylem sap to the shoot (Aroca et al. 2012; Herrera 2013).

Besides that, stomatal conductance (g_s; Fig. 4c, d) is affected, limiting the diffusion of CO_2 from the air into the carboxylation sites of Rubisco enzyme (Ahmed et al. 2002; Bansal and Srivastava 2015), limiting CO_2 fixation (Fig. 4a, b) in all genotypes. On the other hand, intercellular CO_2 concentration increases (C_i; Fig. 4e, f) due to increase in the respiration rate though CO_2 is not used for Rubisco once there is a limited NADPH production caused by a blockage in the ETC of the PSII (Figs. 2, 3). The limited NADPH and ATP produced by the photosynthetic ETC is then dissipated via photorespiration (Fig. 5), contributing to increasing C_i (Fig. 4e, f), observed in common bean plants under flooding. Dissipation of the reducing power and adenylate energy charge through photorespiration is commonly reported in pants under stress (Bräutigam and Gowik 2016). Thus, as the activity of the enzyme GO (estimation of photorespiration) remained constant in plants of cv. BRS Expedito under flooding (Fig. 5), this process may be operating in this cultivar to alleviate the effects caused by stress flooding, while

it does not operate well as evidenced by a decline in the GO activity in other genotypes (Iraí, TB 02–24 and TB 03–13).

Studies with the *Arabidopsis thaliana* suggested that the cyclic transport of electrons around the PSI may help the production of ATP (Tikkanen et al. 2014). This process may be functioning in BRS Expedito, once photorespiration is a process that requires a higher ATP/NADPH ratio (Foyer et al. 2012). Cyclic transport of electrons around PSI to increase ATP production is supported by an increase in ϕ_{Ro} under flooding conditions in BRS Expedito, while this parameter remained similar to the control in Iraí, TB 02–24 and TB 03–13 (Fig. 2c, d).

The genotypes Iraí, TB 02–24 and TB 03–13 presented the value of δ_{Ro} under flooding equal to that found in control plants (normóxia). This may be due to maintenance in the lower production of NADPH by the ETC, also demonstrated by the higher rate of reduction of the final electron acceptors of the PSI (W_{IP}). Thus, NADPH production would help the induction and maintenance of the activity of the enzyme of the ascorbate–glutathione cycle (APX enzyme; Fig. 7e, f) to cope with the effects caused by ROS in flooded plants (Blokhina and Fagerstedt 2010).

The decrease in ET_0/RC due to the blockage in ETC allows electron leakage and ROS production, once there is an increase in TR_0/RC (Fig. 2). The higher production of ROS, such hydrogen peroxide (Fig. 6a, b) and possibly anion superoxide, trigger oxidative damage to lipid membrane, causing lipid peroxidation, as observed in all genotypes (Fig. 6c, d), leading to membrane injuries, protein degradation and enzyme inactivation (Gill and Tuteja 2010). The content of hydrogen peroxide is also a result of the detoxification of superoxide produced by the photosystems due to the activity of SOD (Gill and Tuteja 2010), in Iraí, TB 02–24 and TB 03–13 (Fig. 7a, b), and via GO activity in BRS Expedito (photorespiration; Fig. 5), in peroxisome (Bräutigam and Gowik 2016). In addition to the direct production of H_2O_2 via a pool of plastoquinones (Gururani et al. 2015; Ivanov et al. 2018), in all genotypes.

Moreover, the antioxidative enzyme system is better activated/induced in Iraí, TB 02–24 and TB 03–13 in comparison to BRS Expedito. These genotypes induce more efficiently the activity of SOD, APX, CAT, and GPOD (Fig. 7a–h) to scavenge the ROS produced during the period of flooding (Fig. 6a–d). Differences between common bean genotypes under flooding conditions were reported by Aydogan and Turhan (2015) regarding antioxidative enzymes, besides that, we suppose that these variations resulted from the breeding process resulting in the cv. plants, like BRS Expedito, in contrast with landrace plants. Among the antioxidative enzymes, SOD is the main enzyme that acts on the detoxification of superoxide in H_2O_2. H_2O_2 is then converted to O_2 and H_2O via the action of CAT or H_2O by the action of APX (via ascorbate–glutathione cycle) or GPOD (Azevedo Neto et al. 2006; Gill and Tuteja 2010; Ivanov et al. 2018), to mitigate damages such as lipid peroxidation, verified by the quantification of MDA–TBA (Figs. 6, 7).

Therefore, flooding of the root system may reduce the hydraulic conductivity of water to the shoot, leading to a reduction in stomatal conductance and transpiration rate which impair CO_2 assimilation in leaves of all genotypes. Further, the dynamic energy dissipation of the excess absorbed energy by the photosynthetic ETC is differentially dissipated in all four common bean genotypes. BRS Expedito genotype has a greater energy dissipation through fluorescence and heat over Iraí, TB 02–24 and TB 03–13, with regard of metabolic regulation through photorespiration to alleviate the excess of ATP/NADPH produced by the ETC. On the other hand, the genotypes Iraí, TB 02–24 and TB 03–13 induce more efficiently the antioxidative enzyme system to cope with the deleterious effects of ROS in comparison to BRS Expedito.

Author contribution statement All authors contributed equally to the conception and design of the experiment, acquisition, and analysis of data, drafting and revising the paper.

Acknowledgements This study was financed in part by the Coordenação de Aperfeiçoamento de Pessoal de Nível Superior—Brasil (CAPES)—Finance Code 001 and Conselho Nacional de Desenvolvimento Científico e Tecnológico (CNPq). We are grateful to Embrapa-Terras Baixas and Stoller® for kindly providing common bean seeds and *Rhizobium tropici* strain, respectively.

References

Ahmed S, Nawata E, Sakuratani T (2002) Effects of waterlogging at vegetative and reproductive growth stages on photosynthesis, leaf water potential and yield in mungbean. Plant Prod Sci 5:117–123. https://doi.org/10.1626/pps.5.117

António C, Päpke C, Rocha M, Diab H, Limami AM, Obata T, Fernie AR, van Dongen JT (2016) Regulation of primary metabolism in response to low oxygen availability as revealed by carbon and nitrogen isotope redistribution. Plant Physiol 170:43–56. https://doi.org/10.1104/pp.15.00266

Armstrong W, Strange ME, Cringle S, Beckett PM (1994) Microelectrode and modeling study of oxygen distribution in roots. Ann Bot 74:287–299. https://doi.org/10.1006/anbo.1994.1120

Aroca R, Porcel R, Ruiz-Lozano JM (2012) Regulation of root water uptake under abiotic stress conditions. J Exp Bot 63:43–57. https://doi.org/10.1093/jxb/err266

Aydogan C, Turhan E (2015) Changes in morphological and physiological traits and stress-related enzyme activities of green bean (*Phaseolus vulgaris* L.) genotypes in response to waterlogging stress and recovery treatment. Hort Environ Biotechnol 56:391–401. https://doi.org/10.1007/s13580-015-0127-9

Azevedo Neto AD, Prisco JT, Eneas Filho J, de Abreu CEB, Gomes Filho E (2006) Effect of salt stress on antioxidative enzymes and

lipid peroxidation in leaves and roots of salt-tolerant and salt-sensitive maize genotypes. Environ Exp Bot 56:87–94. https://doi.org/10.1016/j.envexpbot.2005.01.008

Bai YR, Yang P, Su YY, He ZL, Ti XN (2014) Effect of exogenous methanol on glycolate oxidase and photorespiratory intermediates in cotton. J Exp Bot 65:5331–5338. https://doi.org/10.1093/jxb/eru294

Bailey-Serres J, Fukao T, Gibbs DJ, Holdsworth MJ, Lee SC, Licausi F, Perata P, Voesenek LACJ, van Dongen JT (2012) Making sense of low oxygen sensing. Trends Plant Sci 17:129–138. https://doi.org/10.1016/j.tplants.2011.12.004

Bansal R, Srivastava JP (2015) Effect of waterlogging on photosynthetic and biochemical parameters in pigeon pea. Russ J Plant Physiol 62:322–327. https://doi.org/10.1134/S1021443715030036

Blokhina O, Fagerstedt KV (2010) Oxidative metabolism, ROS and NO under oxygen deprivation. Plant Physiol Biochem 48:359–373. https://doi.org/10.1016/j.plaphy.2010.01.007

Borella J, Oliveira HC, Oliveira DDSC, Braga EJB, de Oliveira ACB, Sodek L, do Amarante L (2017) Hypoxia-driven changes in glycolytic and tricarboxylic acid cycle metabolites of two nodulated soybean genotypes. Environ Exp Bot 133:118–127. https://doi.org/10.1016/j.envexpbot.2016.10.007

Bräutigam A, Gowik U (2016) Photorespiration connects C3 and C4 photosynthesis. J Exp Bot 67:2953–2962. https://doi.org/10.1093/jxb/erw056

Cakmak I, Horst WJ (1991) Effect of aluminium on lipid peroxidation, superoxide dismutase, catalase, and peroxidase activities in root tips of soybean (*Glycine max*). Physiol Plant 83:463–468. https://doi.org/10.1111/j.1399-3054.1991.tb00121.x

Cassol D, De Silva FSP, Falqueto AR, Bacarin MA (2008) An evaluation of non-destructive methods to estimate total chlorophyll content. Photosynthetica 46:634–636. https://doi.org/10.1007/s11099-008-0109-6

Eullaffroy P, Frankart C, Aziz A, Couderchet M, Blaise C (2009) Energy fluxes and driving forces for photosynthesis in *Lemna minor* exposed to herbicides. Aquat Bot 90:172–178. https://doi.org/10.1016/j.aquabot.2008.09.002

Foyer CH, Neukermans J, Queval G, Noctor G, Harbinson J (2012) Photosynthetic control of electron transport and the regulation of gene expression. J Exp Bot 63:637–661. https://doi.org/10.1093/jxb/ers013

Foyer CH, Ruban AV, Noctor G (2017) Viewing oxidative stress through the lens of oxidative signaling rather than damage. Biochem J 474:877–883. https://doi.org/10.1042/BCJ20160814

Gill SS, Tuteja N (2010) Reactive oxygen species and antioxidant machinery in abiotic stress tolerance in crop plants. Plant Physiol Biochem 48:909–930. https://doi.org/10.1016/j.plaphy.2010.08.016

Gururani MA, Venkatesh J, Ganesan M, Strasser RJ, Han Y, Kim JI, Lee HY, Song PS (2015) In vivo assessment of cold tolerance through chlorophyll-a fluorescence in transgenic zoysia grass expressing mutant phytochrome A. PLos One 10:e0127200. https://doi.org/10.1371/journal.pone.0127200

Hanawa H, Ishizaki K, Nohira K, Takagi D, Shimakawa G, Sejima T, Shaku K, Makino A, Miyake C (2017) Land plants drive photorespiration as higher electron-sink: comparative study of post-illumination transient O_2-uptake rates from liverworts to angiosperms through ferns and gymnosperms. Physiol Plant 161:138–149. https://doi.org/10.1111/ppl.12580

Herrera A (2013) Responses to flooding of plant water relations and leaf gas exchange in tropical tolerant trees of a blackwater wetland. Front Plant Sci 4:1–12. https://doi.org/10.3389/fpls.2013.00106

Hoagland DR, Arnon DI (1938) The water culture method for growing plants without soil. Cal Agric Exp Stn 347:1–39

Ivanov BN, Borisova-Mubarakshina MM, Kozuleva MA (2018) Formation mechanisms of superoxide radical and hydrogen peroxide in chloroplasts, and factors determining the signaling by hydrogen peroxide. Funct Plant Biol 45:102–110. https://doi.org/10.1071/FP16322

Kreuzwieser J, Rennenberg H (2014) Molecular and physiological responses of trees to waterlogging stress. Plant Cell Environ 37:2245–2259. https://doi.org/10.1111/pce.12310

Lanza LNM, Lanza DCF, Sodek L (2014) Utilization of $^{15}NO_3^-$ by nodulated soybean plants under conditions of root hypoxia. Physiol Mol Biol Plants 20:287–293. https://doi.org/10.1007/s12298-014-0241-7

Limami A, Diab H, Lothier J (2014) Nitrogen metabolism in plants under low oxygen stress. Planta 239:531–541. https://doi.org/10.1007/s00425-013-2015-9

Mielke MS, Schaffer B (2011) Effects of soil flooding and changes in light intensity on photosynthesis of *Eugenia uniflora* L. seedlings. Acta Physiol Plant 33:1661–1668. https://doi.org/10.1007/s11738-010-0702-8

Osorno J, Endres G, Ashley R, Kandel H, Berglund D (2014) Dry bean production guide. NDSU Agriculture, Fargo, 144 p

Rocha M, Licausi F, Araújo WL, Nunes-Nesi A, Sodek L, Fernie AR, van Dongen JT (2010) Glycolysis and the tricarboxylic acid cycle are linked by alanine aminotransferase during hypoxia induced by waterlogging of *Lotus japonicus*. Plant Physiol 152:1501–1513. https://doi.org/10.1104/pp.109.150045

Santos Junior UM, Gonçalves JFC, Strasser RJ, Fearnside PM (2015) Flooding of tropical forests in central Amazonia: what do the effects on the photosynthetic apparatus of trees tell us about species suitability for reforestation in extreme environments created by hydroelectric dams? Acta Physiol Plant 37:1–17. https://doi.org/10.1007/s11738-015-1915-7

Stirbet A, Govindjee (2011) On the relation between the Kautsky effect (chlorophyll a fluorescence induction) and photosystem II: basics and applications of the OJIP fluorescence transient. J Photochem Photobiol B Biol 104:236–257. https://doi.org/10.1016/j.jphotobiol.2010.12.010

Strasser BJ, Strasser RJ (1995) Measuring fast fluorescence transients to address environmental questions: the JIP-test. In: Mathis P (ed) Photosynthesis: from light to biosphere. Kluwer Academic Publishers, Montpellier, pp 977–980

Strasser RJ, Tsimilli-Michael M, Srivastava A (2004) Analysis of the chlorophyll a fluorescence transient. In: Papageorgiou GC, Govindjee (eds) Chlorophyll a fluorescence: a signature of photosynthesis. Spring, Dordrecht, pp 321–362

Tikkanen M, Mekala NR, Aro EM (2014) Photosystem II photoinhibition-repair cycle protects photosystem I from irreversible damage. Biochim Biophys Acta 1837:210–215. https://doi.org/10.1016/j.bbabio.2013.10.001

Tsimilli-Michael M, Strasser RJ (2008) In vivo assessment of plants vitality: applications in detecting and evaluating the impact of mycorrhization on host plants. In: Varma A (ed) Mycorrhiza. Dordrecht: Springer, 3rd ed., 679–703

van Dongen JT, Licausi F (2015) Oxygen sensing and signalling. Annu Rev Plant Biol 66:345–367. https://doi.org/10.1146/annurev-arplant-043014-114813

Velikova V, Yordanov I, Edreva A (2000) Oxidative stress and some antioxidant systems in acid rain-treated bean plants. Plant Sci 151:59–66. https://doi.org/10.1016/S0168-9452(99)00197-1

Yan K, Chen P, Shao H, Shao C, Zhao S, Brestic M (2013) Dissection of photosynthetic electron transport process in sweet sorghum under heat stress. Plos One 8:special issue 62100. https://doi.org/10.1371/journal.pone.0062100

Yusuf MA, Kumar D, Rajwanshi R, Strasser RJ, Tsimilli-Michael M, Govindjee; Sarin NB (2010) Overexpression of γ-tocopherol methyl transferase gene in transgenic *Brassica juncea* plants

alleviate abiotic stress: physiological and chlorophyll *a* fluorescence measurements. Biochim Biophys Acta Bioenerg 1797:428–1438. https://doi.org/10.1016/j.bbabio.2010.02.002

United States Department of Agriculture (USDA) (2015) Hearing: agriculture's role in combatting global hunger. U.S. Government Publishing Office, Washington, p 126